Article:
Tych, KM, Wood, CD, Burnett, AD et al. (2014) Probing temperature- and solvent-dependent protein dynamics using terahertz time-domain spectroscopy. Journal of Applied Crystallography, 47 (1). 146 - 153. ISSN: 0021-8898

https://doi.org/10.1107/S1600576713029506

Journal of
Applied Crystallography
ISSN 1600-5767

Probing temperature- and solvent-dependent protein dynamics using terahertz time-domain spectroscopy

Katarzyna M. Tych, Christopher D. Wood, Andrew D. Burnett, Arwen R. Pearson, A. Giles Davies, Edmund H. Linfield and John E. Cunningham

J. Appl. Cryst. (2014). **47**, 146–153

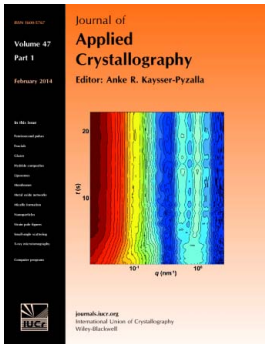

Many research topics in condensed matter research, materials science and the life sciences make use of crystallographic methods to study crystalline and non-crystalline matter with neutrons, X-rays and electrons. Articles published in the *Journal of Applied Crystallography* focus on these methods and their use in identifying structural and diffusion-controlled phase transformations, structure-property relationships, structural changes of defects, interfaces and surfaces, *etc.* Developments of instrumentation and crystallographic apparatus, theory and interpretation, numerical analysis and other related subjects are also covered. The journal is the primary place where crystallographic computer program information is published.

Journal of
Applied Crystallography
ISSN 1600-5767

Received 22 May 2013
Accepted 25 October 2013

Probing temperature- and solvent-dependent protein dynamics using terahertz time-domain spectroscopy

Katarzyna M. Tych, Christopher D. Wood, Andrew D. Burnett, Arwen R. Pearson,* A. Giles Davies, Edmund H. Linfield and John E. Cunningham*

Astbury Centre for Structural Molecular Biology, University of Leeds, Woodhouse Lane, Leeds LS2 9JT, UK. Correspondence e-mail: a.r.pearson@leeds.ac.uk, j.e.cunningham@leeds.ac.uk

The effect of temperature on the terahertz-frequency-range material properties of lyophilized and single-crystal hen egg-white lysozyme has been measured using terahertz time-domain spectroscopy, with the results presented and discussed in the context of protein and solvent dynamical and glass transitions. Lyophilized hen egg-white lysozyme was measured over a temperature range from 4 to 290 K, and a change in the dynamical behaviour of the sample at around 100 K was observed through a change in the terahertz absorption spectrum. Additionally, the effect of cryoprotectants on the temperature-dependent absorption coefficient is studied, and it is demonstrated that terahertz time-domain spectroscopy is capable of resolving the true glass transition temperature of single-crystal hen egg-white lysozyme at ∼150 K, which is in agreement with literature values measured using differential scanning calorimetry.

1. Introduction

The study of the effects of temperature and hydration on protein molecules is critical to understanding both the contribution of dynamics to protein function and the interaction between proteins and their surrounding aqueous environment (Gabel *et al.*, 2002; Rupley & Careri, 1991; Weik, 2003). Functionally related dynamics of protein molecules, such as those involved in ligand binding and signalling, are associated with the fast thermal fluctuations of amino acid side chains, which occur on time scales between pico- and nanoseconds. These time scales overlap with those probed by terahertz time-domain spectroscopy (THz-TDS) (from 0.14 to 3.3 ps in this work).

The electric field of the THz radiation will interact with motions within the system that cause a change in dipole moment (Decius & Hexter, 1977). In simple molecular crystals this has been shown to take the form of a summation of low-frequency harmonic normal modes, which can be approximated by Lorentzian dipoles (Burnett *et al.*, 2013; Lipps *et al.*, 2012). In liquids or amorphous systems that show no long-range order, and thus no low-frequency collective vibrational normal modes, rotational motions on these time scales are linked with the dielectric permittivity of the system and are often represented by a summation of Debye relaxations (Schröder & Steinhauser, 2010; Lipps *et al.*, 2012) or a Havriliak–Negami function (Schröder & Steinhauser, 2010; Sun *et al.*, 2012; Sibik *et al.*, 2013). The translation counterpart to the dielectric permittivity is known as the dielectric conductivity and will further contribute to the observed THz dielectric response (Schröder & Steinhauser, 2010; Lloyd-Hughes & Jeon, 2012). It should also be noted that the observed THz dielectric spectrum will not simply be a summation of its component parts but in fact a complex mixture which can often only be decomposed using an effective medium theory (Vinh *et al.*, 2011), if the dielectric response of many of its component parts are already known. Thus the observed THz spectrum is a complex measure of the vibrational and relaxational processes occurring over a time scale of 100 fs to ∼4 ps. Even in the case of THz spectra of bulk water, there is much discussion as to whether a double or triple Debye model is best, or whether harmonic Lorentz resonances should also be included (Beneduci, 2008). In fact it is often very difficult to deconvolve the components of the spectra without complex theoretical calculations (Schröder & Steinhauser, 2010). THz-TDS has, however, been previously used to study proteins in solution (Luong *et al.*, 2011), hydrated thin films (Knab *et al.*, 2007; Whitmire *et al.*, 2003), dry powders (Markelz *et al.*, 2002; Zhang *et al.*, 2004) and, recently, the single-crystal form (Tych *et al.*, 2011). The results of these studies have demonstrated the sensitivity of THz-TDS to light-activated conformational changes in photoactive proteins (Castro-Camus & Johnston, 2008), the ability to distinguish between proteins in the wild-type form and those with single-point mutations (Whitmire *et al.*, 2003), and the detection of functionally related hydration- and temperature-dependent transitions in the dielectric properties of protein samples (Markelz *et al.*, 2007). The temperature-dependent change at ∼180 K in proteins is often referred to as the

'protein glass transition' (Green *et al.*, 1994; Ringe & Petsko, 2003); for clarity, in this article we will refer to this as a 'dynamical transition' instead (Doster *et al.*, 1989), to distinguish it from a true glass transition.

In our work, variable-temperature measurements of hen egg-white lysozyme (HEWL) crystals were performed using THz-TDS, employing both cryoprotected and unprotected single crystals, to assess whether the true glass transition and dynamical transitions of these crystals can be detected using THz-TDS. Variable-temperature measurements of protein single crystals of HEWL were conducted at temperatures from 127 to 290 K using a nitrogen-cooled cryostream. We also performed complementary measurements on lyophilized HEWL pellets over a temperature range from 4 to 290 K using a continuous-flow helium-cooled microstat.

2. Materials and methods

The experimental arrangement used for THz-TDS in this work was as previously described (Tych *et al.*, 2011). The entire THz beam path was inside a dry-air-purged sealed container, to prevent water vapour absorption from influencing the resulting sample spectrum.

For pressed pellet samples, lyophilized HEWL powder (three times crystallized, Sigma–Aldrich, UK) was used without further purification. Pellets with concentrations of 25, 50, 75 and 100%(*w*/*w*) HEWL were prepared using 1 µm particle size polytetrafluoroethylene (PTFE, Sigma–Aldrich) as a matrix material. The matrix material, which has very low absorption in the THz frequency range, was used to dilute the highly absorbing protein sample. This concentration series was used in order to determine the maximum concentration of protein in the pressed pellet sample before the detected THz signal dropped below the noise floor of the system, as is standard. The protein and matrix mixtures were pressed into copper rings as described in earlier work (Shen *et al.*, 2004). Pellets were immediately mounted inside the dry-air-purged box, maintaining the hydration level at that of a lyophilized powder. They were positioned in a continuous-flow helium-cooled cryostat (He-Microstat, Oxford Instruments, UK), providing temperature control between 4 and 290 K. The temperature step size in the measurements was 10 K (except for the first step from 4 to 20 K). The measurement at each temperature step was recorded in triplicate and took 3 min.

For protein single crystals, HEWL (Sigma–Aldrich, three times crystallized) was used without further purification and dissolved in 0.1 *M* sodium acetate buffer pH 4.8, to a concentration of 50 mg ml^{-1}. Sitting-drop vapour diffusion crystallization was then performed [0.1 *M* sodium acetate buffer pH 4.7–5.0, 8%(*w*/*v*) with NaCl as the precipitant] using 10 µl drops, comprising 5 µl of protein solution and 5 µl of reservoir solution, following an established protocol (Alderton & Fevold, 1946). Tetragonal crystals with volumes ranging from ∼0.05 to ∼1 mm^3 were obtained within three weeks. Tetragonal HEWL crystals have a solvent content of 36.31%, calculated using the Matthews (1968) coefficient, with solvent channels of between 1 and 2.5 nm in diameter (Falkner *et al.*, 2005).

Half of the HEWL crystals were cryoprotected by submerging them for 60 s in a droplet containing 20%(*v*/*v*) glycerol in reservoir solution from the well above which the crystal was grown. The crystals were transferred using mounted cryoloops (Hampton Research) onto the surface of a pinhole aperture (300 µm diameter, Edmund Optics), and excess liquid was removed, before they were flash cooled under the nitrogen cryostream (Oxford Cryosystems) at a temperature of 127 K. The purged atmosphere prevented crystallization of water from the surrounding air on the surface of the sample. The cryostream provided sample temperatures between 127 and 290 K. The temperature of the metal aperture at the sample position was calibrated using a PT100 thin-film temperature sensor (126–6923, Farnell, UK). The position of the pinhole aperture was then optimized for maximum THz transmission. The dimensions of each crystal were measured prior to being mounted on the aperture.

The THz dielectric properties of the measured samples can be described by the frequency-dependent absorption coefficient [$\alpha(\nu)$, mm^{-1}], obtained from the Beer–Lambert law as previously described (Tych *et al.*, 2011). This absorption coefficient was extracted from a fast Fourier transform of the time-domain electric field transmitted through the sample and from reference measurements of either free space for pelleted samples or the pinhole aperture for the crystal measurements. In order to calibrate the dynamic range of the experimental setup, the maximum detectable absorption coefficient $\alpha_{\max}$, over all frequencies, was calculated for the thickness and refractive index of each sample, using a method previously described by Uhd Jepsen & Fischer (2005). For samples where the thickness could not be easily measured, in which only relative changes in material properties were of interest, we have calculated an extinction coefficient rather than a true absorption coefficient (Zhong *et al.*, 2006).

3. Results

3.1. Pressed pellet samples

Pellets of each HEWL concentration [25, 50, 75 and 100%(*w*/*w*)] were measured. The absorption coefficient of a 50%(*w*/*w*) HEWL pellet is shown in Fig. 1, as an example. Unlike similar variable-temperature spectra obtained for small-molecule samples (Fan *et al.*, 2007), there are no clear absorption peaks present in the pellet samples at repeatable spectral positions (supplementary Fig. S5[1]).

Below the frequency cut-off, defined as the maximum detectable absorption coefficient for each pellet (dashed line in Fig. 1), changes were observed in the overall absorption coefficient with increasing temperature: the absorption coefficient at a single frequency for any one temperature was found to increase linearly with the concentration of HEWL in the pellet, as expected from the Beer–Lambert law (Fig. 2*a*).

[1] Supplementary figures for this article are available from the IUCr electronic archives (Reference: FS5051).

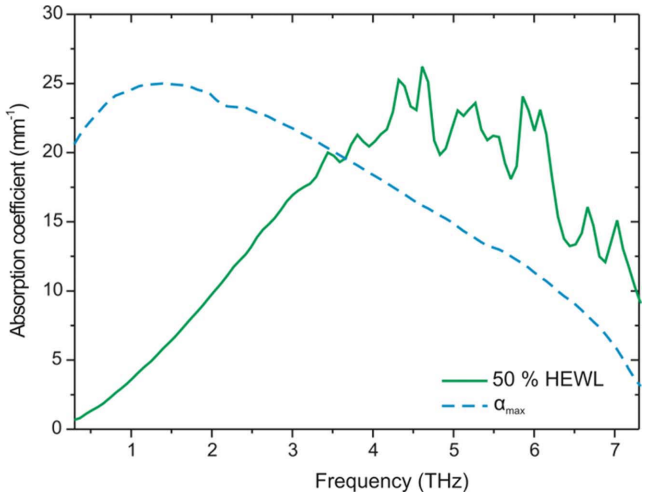

Figure 1
The absorption coefficient for a 50% HEWL, 50% PTFE pellet measured at 4 K showing the detection limit (α_{max}) of the system for this sample, as calculated by Uhd Jepsen & Fischer (2005).

More interestingly, when the absorption coefficient at a single frequency for each concentration is plotted with respect to temperature, a local minimum is found at 80–100 K for all concentrations (Figs. 2*b*–2*d*), with the onset of linear behaviour starting at ∼100 K. We note that this is close to the low-temperature (∼100–120 K) inflection, linked to methyl side-group dynamics, previously observed in proteins using neutron scattering (Roh *et al.*, 2006; Wood *et al.*, 2008). In these studies, Wood *et al.* used deuterated protein but not HEWL, and Roh *et al.* used HEWL that was not deuterated. The slight change in the slope of the temperature-dependent absorption coefficient at around 140 K is not consistently seen at different concentrations and frequencies; therefore we cannot attribute this to a real transition using the data presented here.

HEWL molecules have been shown to expand by up to ∼3% when heated from 95 K up to 295 K (Juers & Matthews, 2001). No data are available for a greater range of temperatures than this, to the authors' knowledge. The change in

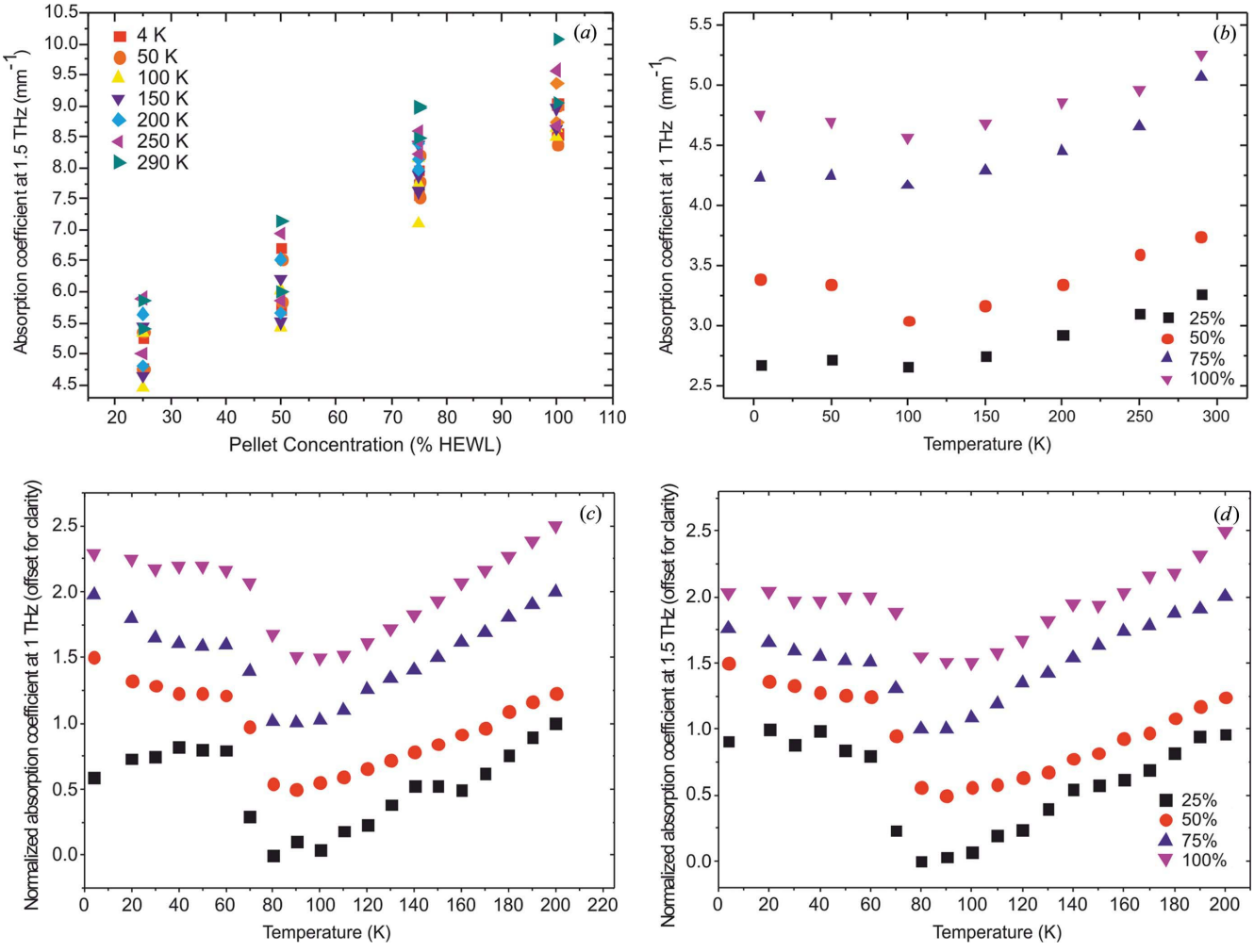

Figure 2
(*a*), (*b*) The absorption coefficients obtained from fast Fourier transforms of time-domain traces from 4 to 290 K: (*a*) two pressed pellets at each concentration of HEWL (25, 50, 75 and 100%), showing the variation in absorption coefficient with concentration, and (*b*) the variation in average absorption coefficient at each concentration with temperature, at 1 THz. (*c*), (*d*) The normalized absorption coefficients obtained from Fourier transformation of time-domain traces from 4 to 200 K of pressed pellets of HEWL at concentrations of 25, 50, 75 and 100% at (*c*) 1 THz and (*d*) 1.5 THz.

absorption coefficient over all concentrations of HEWL is significantly greater than this (the smallest change for a single pellet over the temperature range from 4 K up to 290 K is ∼18%), meaning that the increase in absorption coefficient measured cannot be fully accounted for by changes in the thickness of the pellet. The greatest source of uncertainty in these measurements is not the thermal expansion of the samples but the measurement of the pellet thickness. This gives an uncertainty of ±10% in the calculated absorption coefficient for each pellet. This does not affect the measured relative changes in absorption coefficient for a single pellet with temperature.

3.2. Single-crystal measurements

Owing to experimental restrictions, data could only be recorded between 127 and 290 K for the single-crystal samples (Figs. S3 and S4). The THz frequency-dependent absorption coefficient was calculated, and a sudden increase was observed between 142 and 152 K in the crystals cryoprotected with 20% glycerol (Fig. 3), close to the reported glass transition for a 30% glycerol in water mixture (Harran, 1978; Weik *et al.*, 2004). Transitions at similar temperatures have also been seen using THz-TDS for sorbitol–water mixtures and are proposed to be due to relaxation processes slowing down and shifting out of the spectral window covered by THz-TDS (Sibik *et al.*, 2013). This transition occurred in HEWL crystals in the absence of cryoprotectant at a similar temperature (between 138 and 148 K; Fig. 4), although the transition is less clearly defined. A slight increase in the transition temperature for the cryoprotectant-containing crystals would be in agreement with the difference in glass transition temperatures measured for water and glycerol solutions reported previously (Harran, 1978; Weik *et al.*, 2004). Tsai *et al.* (2000) also showed an increase in the transition temperature when glycerol was used as a solvent for lysozyme, over a range of different concentrations.

The absorption coefficient for each crystal sharply decreases above 160 K (Fig. S1), making it impossible to observe the 180–250 K dynamical transition. We suggest that

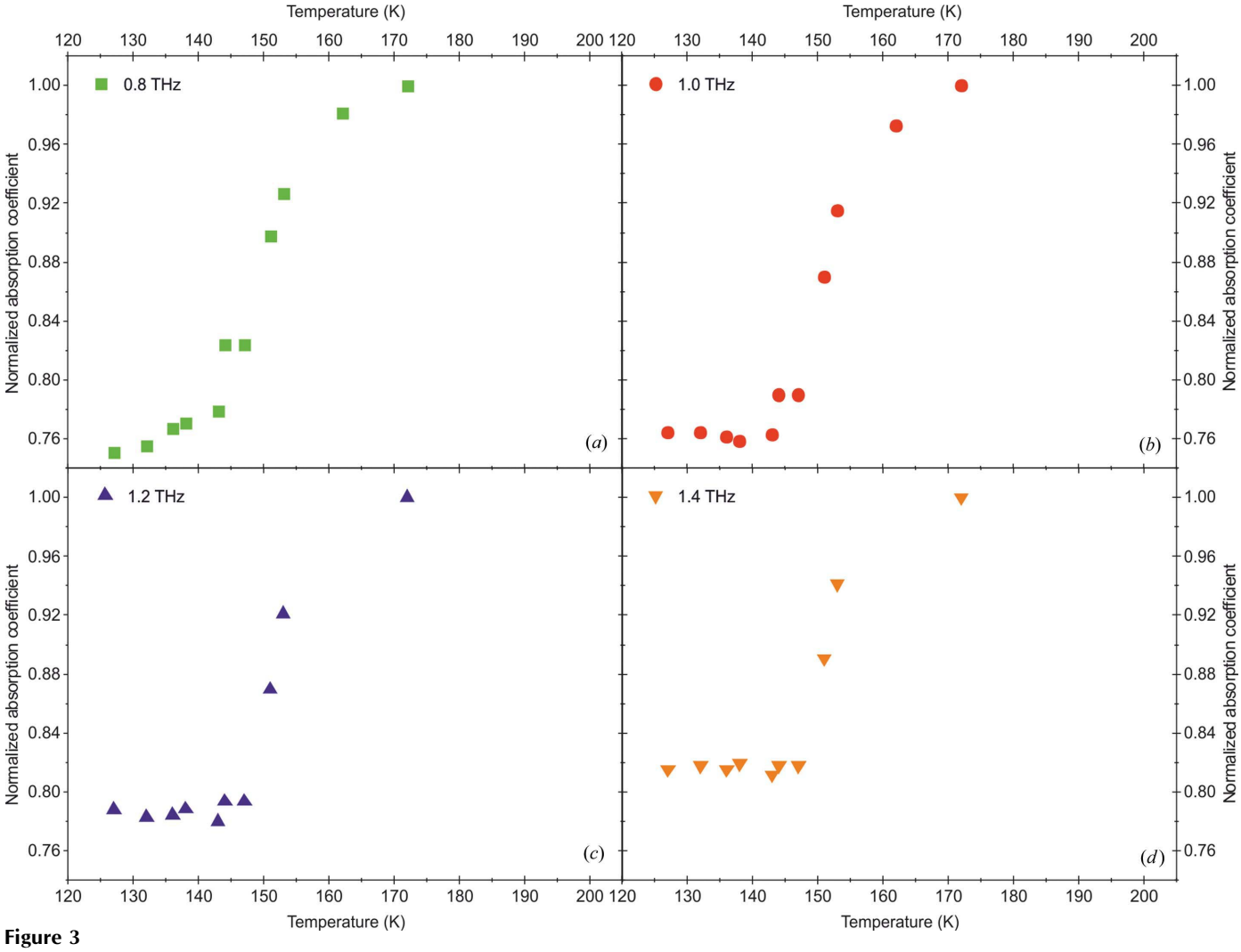

Figure 3
Variable-temperature THz frequency material parameters at 0.8, 1.0, 1.2 and 1.4 THz of a HEWL crystal, cryoprotected with glycerol, measured from 127 to 197 K, showing the normalized absorption coefficient at each frequency.

this drop in absorption corresponds to the onset of bulk solvent sublimation from the crystal. This is supported by our experiments conducted using crystallization mother liquor alone, in which the solution sublimed completely at a temperature of 160 K (manifesting as a drop to zero in the extinction curve; Fig. 5). The slight variation in the temperature (±10 K) at which this sublimation begins is attributed to differences in the crystal size and the level of uncertainty in the temperature measurements (Fig. S2). The data we present in Figs. 3 and 4 are therefore only shown up to the point where the absorption coefficient is at a maximum.

A second set of factors that may influence the changes in absorption coefficient between 127 and 160 K in HEWL crystals are those aspects of solvent and protein behaviour which occur as a result of confinement within a crystal lattice. Generally, flash cooling from room temperature down to 77 K reduces the volume of a protein crystal unit cell by between 2 and 7%, within which the protein molecules contract by between 1 and 3% in volume (Weik & Colletier, 2010; Young *et al.*, 1994; Juers & Matthews, 2001). As a result, an increase in the volume of the protein crystal with increasing temperature, which cannot be accounted for during the THz-TDS measurements, could also contribute to an increase in the absorption coefficient. However, this is not considered the dominant effect as, as in the pellet samples, the percentage change in the absorption coefficient we observe is much greater (between 15 and 30% for all crystals measured, over all frequencies).

4. Discussion

In glass-forming liquids, several material properties, including the viscosity and the heat capacity, undergo marked changes at the glass-transition temperature, T_g (Angell, 1995); at this temperature, molecules that are trapped in a rigid state at lower temperatures become more mobile (Parak, 2003). One useful quantitative measure of dynamic properties frequently used in neutron scattering and Mössbauer spectroscopy, for

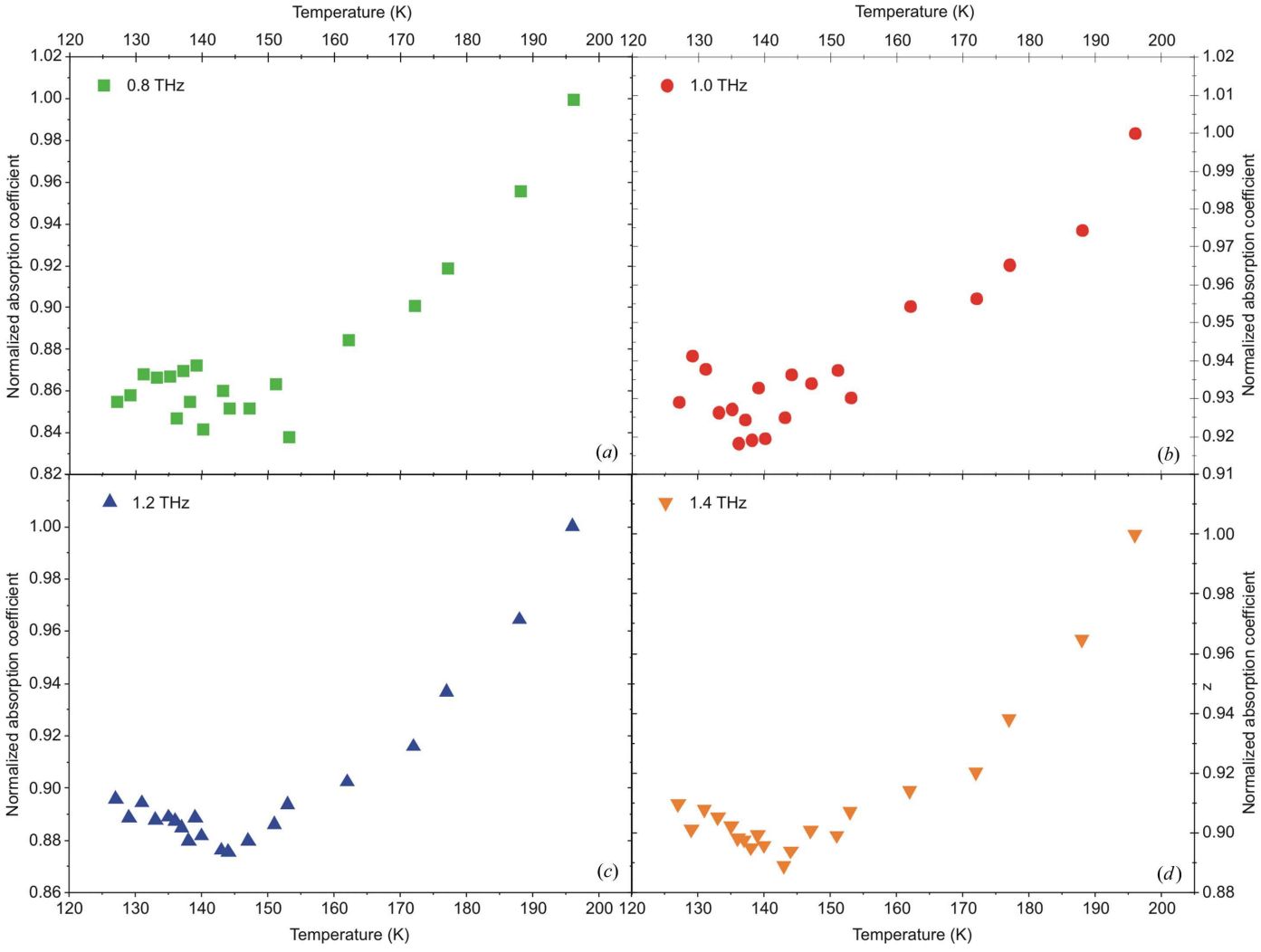

Figure 4
Variable-temperature THz frequency material parameters at 0.8, 1.0, 1.2 and 1.4 THz of an unprotected HEWL crystal, measured from 127 to 197 K, showing the normalized absorption coefficient at each frequency.

example, is the mean square atomic displacement $\langle x^2 \rangle$. A sharp change in $\langle x^2 \rangle$ at a given temperature is an indication that a change in the dynamical behaviour of the sample has occurred. Such sharp changes in $\langle x^2 \rangle$ have been observed in a variety of hydrated proteins (Chong *et al.*, 2001; Ferrand *et al.*, 1993; Mack *et al.*, 2000), polypeptides (Bajaj *et al.*, 2008) and amino acids (Schiró *et al.*, 2011) at temperatures between 180 and 240 K using Mössbauer spectroscopy, nuclear magnetic resonance (NMR) and neutron scattering experiments (Bajaj *et al.*, 2008; Chong *et al.*, 2001; Ferrand *et al.*, 1993; Mack *et al.*, 2000), and at temperatures between 180 and 240 K using THz-TDS (Chen *et al.*, 2005; He *et al.*, 2008). It is important to note that the temperature-dependent changes seen in these studies are not attributed to a true glass transition but rather to a change in the dynamical behaviour of the protein molecules within the sample, with similarities to the changes in material properties of liquids when they form a glass. This transition has been shown to occur in both unfolded and folded proteins, indicating that its existence does not depend on the protein's conformational state (He *et al.*, 2008), although it requires the sample to be at least minimally hydrated, with 0.2 g of water per gram of protein (Roh *et al.*, 2006). The dynamical transition has been linked to the onset of anharmonic protein motion. This is commonly accepted to occur at a temperature determined either by the solvent or the protein – whichever has the higher transition temperature (Réat *et al.*, 2000).

Neutron scattering measurements of several proteins, in which samples were isotopically labelled in order to deconvolve the contributions of the solvent and the sample to the change in $\langle x^2 \rangle$, have demonstrated that the temperature at which this dynamical transition occurs is strongly dependent on the solvent viscosity (Gabel *et al.*, 2002; Tsai *et al.*, 2000). Molecular dynamics simulations further suggest that this dynamical transition is linked to changes in protein–water hydrogen-bonding patterns which occur as the water molecules become more mobile at higher temperature (Tarek & Tobias, 2002). Finally, neutron scattering studies have provided evidence that the increase in protein $\langle x^2 \rangle$ that occurs at the dynamical transition is linked to an onset of biological function in some systems (Ferrand *et al.*, 1993), although work also involving neutron scattering has suggested otherwise (Daniel *et al.*, 1998; Dunn *et al.*, 2000).

There is a second, lower-temperature inflection in $\langle x^2 \rangle$, measured using neutron scattering. This less widely studied inflection has been shown to occur in proteins independently of hydration state, and has been experimentally observed at 100–120 K for lysozyme and 150 K for staphylococcal nuclease (Nakagawa *et al.*, 2008; Roh *et al.*, 2006). Molecular dynamics and normal mode analysis have predicted this inflection for bovine pancreatic trypsin inhibitor (between 100 and 120 K) and myoglobin (150 K) (Hayward & Smith, 2002; Krishnan *et al.*, 2008). The low-temperature inflection appears to be specific to proteins and has not been observed in nucleic acids or solvent alone (Roh *et al.*, 2009). Measurements made using elastic incoherent neutron scattering of isotopically labelled solutions and dry powders of proteins, when combined with molecular dynamics simulations, have resulted in the hypothesis that this low-temperature dynamical transition is linked to the time scales of methyl group rotations entering the experimental time window of the instrument used, meaning that it is not a dynamical transition, as the temperature at which it occurs depends on the instrument used to measure it (Roh *et al.*, 2006; Wood *et al.*, 2010; Doster & Settles, 2005; Schiró *et al.*, 2010). In the HEWL pressed pellet samples studied here, a change in THz response was also observed between 80 and 100 K for all samples, at all frequencies measured.

In protein crystals, studies of the effect of temperature on protein structure and flexibility are complicated by a convolution of the effects of solvent expansion and lattice contraction as well as changes in the bound and bulk solvent (Kurinov & Harrison, 1995; Weik, 2003). The solvent in crystals differs from bulk water both because it is confined by the protein molecules and because it contains solutes such as buffers and

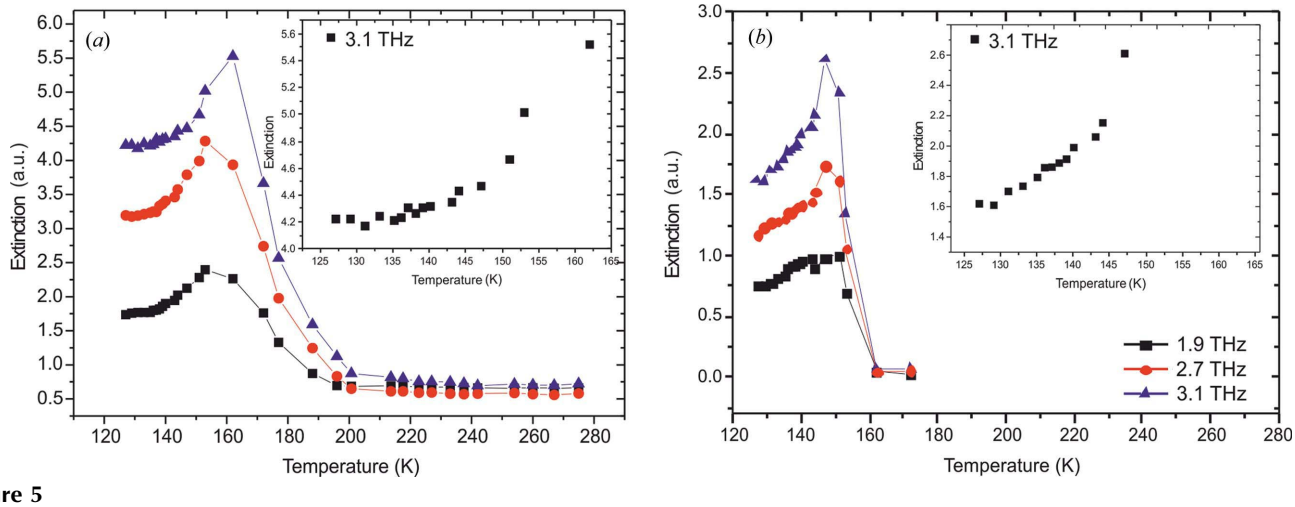

Figure 5
(*a*) Variable-temperature measurement of reservoir solution with 20% glycerol cryoprotectant and (inset) the extinction at a single frequency for the same measurement (3.1 THz) in the 120–150 K region, for clarity. (*b*) Variable-temperature measurement of reservoir solution without cryoprotectant and (inset) the extinction at a single frequency for the same measurement (3.1 THz) in the 120–160 K region, for clarity.

precipitants; this confinement results in a higher viscosity than that of bulk water (Weik & Colletier, 2010). There are two suggested ways in which the solvent can affect protein dynamics: by frictional damping and by modifying the effective potential surface of the protein (Brooks & Karplus, 1989; Réat *et al.*, 2000; Smith *et al.*, 1990). Adding a cryoprotecting solvent such as glycerol, as is routine for low-temperature X-ray diffraction experiments on protein crystals, can increase the viscosity of the bulk solvent in the solvent channels of the crystal, and has been shown in neutron scattering measurements of lysozyme powder to change the temperature at which the second, hydration-dependent, dynamical transition occurs (Tsai *et al.*, 2000).

The transition that we measured in HEWL crystals occurred at a lower temperature than the typically reported dynamical transition for proteins (180–250 K; Bajaj *et al.*, 2008; Chong *et al.*, 2001; Ferrand *et al.*, 1993; Mack *et al.*, 2000; Doster *et al.*, 1989) but is very close to the HEWL crystal true glass transition, T_g, measured by differential scanning calorimetry of HEWL crystals at 150 K (Miyazaki *et al.*, 2000). Neutron scattering studies of HEWL crystals do not include measurements at this temperature (Bon *et al.*, 2002). Differential scanning calorimetry measurements of hydrated thin films of HEWL report a glass-transition temperature between 155 and 170 K, depending on hydration state (Panagopoulou *et al.*, 2011). This true glass transition where a phase change occurs in hydrated thin films has not been reported in neutron scattering studies; therefore a comparison between neutron scattering and THz-TDS is not currently possible. We did not observe this T_g transition in lyophilized lysozyme pellets. However, a transition at this temperature was observed in crystallization mother liquor with and without glycerol, in the absence of protein (Fig. 5). This suggests that the glass transition measured calorimetrically at ∼150 K in HEWL crystals may be solvent mediated. Although the solvent channels in tetragonal lysozyme crystals are not large enough to permit the formation of crystalline ice (over 28 Å) (Weik & Colletier, 2010), it has been shown that water can be transported out of solvent channels over 10 Å in size (Juers & Matthews, 2004) and can then crystallize on the surface of the protein crystal (Weik *et al.*, 2005). As a result, the calorimetrically measured glass transition of the protein crystals at ∼150 K may be related to the onset of the crystallization of water that has been transported out of the protein crystal solvent channels (Weik & Colletier, 2010).

5. Conclusions

We have presented THz-TDS measurements of pressed pellets of lyophilized HEWL and protein single crystals of HEWL, both of which reveal changes in the absorption coefficient as a function of temperature that correlate with known transitions.

It is important to consider the two sets of samples, the crystals and the pellets, separately, since the pressed pellets of lyophilized HEWL are amorphous and virtually dehydrated. They therefore have very different THz absorption properties from HEWL crystals, which contain a large amount of solvent within their channels and where the protein molecules are arranged in a crystalline structure. The observed transitions are also different in nature – whilst the low-temperature change in dynamical behaviour in the lyophilized pressed pellets may be related to the known low-temperature inflection in $\langle x^2 \rangle$, the higher-temperature transition seen in the crystal samples correlates to the known phase transition or true glass transition of tetragonal HEWL crystals. As samples undergoing both types of transition exhibit a change in THz frequency dynamics it is possible to measure both using THz-TDS.

The authors are grateful for the support of the EPSRC, the Leverhulme Trust, the Royal Society and the Wolfson Foundation. The authors thank Martin Weik for critical discussion of the manuscript.

References

Alderton, G. & Fevold, H. L. (1946). *J. Biol. Chem.* **164**, 1–5.
Angell, C. A. (1995). *Science*, **267**, 1924–1935.
Bajaj, V. S., van der Wel, P. C. A. & Griffin, R. G. (2008). *J. Am. Chem. Soc.* **131**, 118–128.
Beneduci, A. (2008). *J. Mol. Liq.* **138**, 55–60.
Bon, C., Dianoux, A. J., Ferrand, M. & Lehmann, M. S. (2002). *Biophys. J.* **83**, 1578–1588.
Brooks, C. L. & Karplus, M. (1989). *J. Mol. Biol.* **208**, 159–181.
Burnett, A. D., Kendrick, J., Russell, C., Christensen, J., Cunningham, J. E., Pearson, A. R., Linfield, E. H. & Davies, A. G. (2013). *Anal. Chem.* **85**, 7926–7934.
Castro-Camus, E. & Johnston, M. (2008). *Chem. Phys. Lett.* **455**, 289–292.
Chen, J., Knab, J., Cerne, J. & Markelz, A. (2005). *Phys. Rev. E*, **72**, 040901.
Chong, S. H., Joti, Y., Kidera, A., Go, N., Ostermann, A., Gassmann, A. & Parak, F. (2001). *Eur. Biophys. J.* **30**, 319–329.
Daniel, R. M., Smith, J. C., Ferrand, M., Héry, S., Dunn, R. & Finney, J. L. (1998). *Biophys. J.* **75**, 2504–2507.
Decius, J. C. & Hexter, R. M. (1977). *Molecular Vibrations in Crystals.* New York: McGraw-Hill.
Doster, W., Cusack, S. & Petry, W. (1989). *Nature*, **337**, 754–756.
Doster, W. & Settles, M. (2005). *Biochim. Biophys. Acta Proteins Proteomics*, **1749**, 173–186.
Dunn, R. V., Réat, V., Finney, J., Ferrand, M., Smith, J. C. & Daniel, R. M. (2000). *Biochem. J.* **346**, 355–358.
Falkner, J. C., Al-Somali, A. M., Jamison, J. A., Zhang, J., Adrianse, S. L., Simpson, R. L., Calabretta, M. K., Radding, W., Phillips, G. N. & Colvin, V. L. (2005). *Chem. Mater.* **17**, 2679–2686.
Fan, W. H., Burnett, A., Upadhya, P. C., Cunningham, J., Linfield, E. H. & Davies, A. G. (2007). *Appl. Spectrosc.* **61**, 638–643.
Ferrand, M., Petry, W., Dianoux, A. & Zaccai, G. (1993). *Physica A*, **201**, 425–429.
Gabel, F., Bicout, D., Lehnert, U., Tehei, M., Weik, M. & Zaccai, G. (2002). *Q. Rev. Biophys.* **35**, 327–367.
Green, J. L., Fan, J. & Angell, C. A. (1994). *J. Phys. Chem.* **98**, 13780–13790.
Harran, D. (1978). *Bull. Soc. Chim. Fr.* **1–2**, 40–44.
Hayward, J. A. & Smith, J. C. (2002). *Biophys. J.* **82**, 1216–1225.
He, Y., Ku, P. I., Knab, J. R., Chen, J. Y. & Markelz, A. G. (2008). *Phys. Rev. Lett.* **101**, 178103.
Juers, D. H. & Matthews, B. W. (2001). *J. Mol. Biol.* **311**, 851–862.
Juers, D. H. & Matthews, B. W. (2004). *Acta Cryst.* D**60**, 412–421.
Knab, J. R., Chen, J., He, Y. & Markelz, A. G. (2007). *Proc. IEEE*, **95**, 1605–1610.

Krishnan, M., Kurkal-Siebert, V. & Smith, J. C. (2008). *J. Phys. Chem. B*, **112**, 5522–5533.
Kurinov, I. V. & Harrison, R. W. (1995). *Acta Cryst.* D**51**, 98–109.
Lipps, F., Levy, S. & Markelz, A. G. (2012). *Phys. Chem. Chem. Phys.* **14**, 6375–6381.
Lloyd-Hughes, J. & Jeon, T.-I. (2012). *J. Infrared Millimeter Terahertz Waves*, **33**, 871–925.
Luong, T. Q., Verma, P. K., Mitra, R. K. & Havenith, M. (2011). *Biophys. J.* **101**, 925–933.
Mack, J. W., Usha, M. G., Long, J., Griffin, R. G. & Wittebort, R. J. (2000). *Biopolymers*, **53**, 9–18.
Markelz, A. G., Knab, J. R., Chen, J. Y. & He, Y. (2007). *Chem. Phys. Lett.* **442**, 413–417.
Markelz, A. G., Whitmire, S. E., Hillebrecht, J. R. & Birge, R. R. (2002). *Phys. Med. Biol.* **47**, 3797–3805.
Matthews, B. W. (1968). *J. Mol. Biol.* **33**, 491–497.
Miyazaki, Y., Matsuo, T. & Suga, H. (2000). *J. Phys. Chem. B*, **104**, 8044–8052.
Nakagawa, H., Joti, Y., Kitao, A. & Kataoka, M. (2008). *Biophys. J.* **95**, 2916–2923.
Panagopoulou, A., Kyritsis, A., Aravantinou, A., Nanopoulos, D., i Serra, R., Gómez Ribelles, J., Shinyashiki, N. & Pissis, P. (2011). *Food Biophys.* **6**, 199–209.
Parak, F. G. (2003). *Rep. Prog. Phys.* **66**, 103–129.
Réat, V., Dunn, R., Ferrand, M., Finney, J. L., Daniel, R. M. & Smith, J. C. (2000). *Proc. Natl Acad. Sci. USA*, **97**, 9961–9966.
Ringe, D. & Petsko, G. A. (2003). *Biophys. Chem.* **105**, 667–680.
Roh, J. H., Briber, R. M., Damjanovic, A., Thirumalai, D., Woodson, S. A. & Sokolov, A. P. (2009). *Biophys. J.* **96**, 2755–2762.
Roh, J. H., Curtis, J. E., Azzam, S., Novikov, V. N., Peral, I., Chowdhuri, Z., Gregory, R. B. & Sokolov, A. P. (2006). *Biophys. J.* **91**, 2573–2588.
Rupley, J. A. & Careri, G. (1991). *Advances in Protein Chemistry*, edited by C. B. Anfinsen, F. M. Richards, J. T. Edsall & S. E. David, Vol. 41, pp. 37–172. Waltham: Academic Press.
Schiró, G., Caronna, C., Natali, F. & Cupane, A. (2010). *J. Am. Chem. Soc.* **132**, 1371–1376.
Schiró, G., Caronna, C., Natali, F., Koza, M. M. & Cupane, A. (2011). *J. Phys. Chem. Lett.* **2**, 2275–2279.
Schröder, C. & Steinhauser, O. (2010). *Computational Spectroscopy*, pp. 279–321. Weinheim: Wiley-VCH Verlag.
Shen, Y. C., Upadhya, P. C., Linfield, E. H. & Davies, A. G. (2004). *Vib. Spectrosc.* **35**, 111–114.
Sibik, J., Shalaev, E. Y. & Axel Zeitler, J. (2013). *Phys. Chem. Chem. Phys.* **15**, 11931–11942.
Smith, J., Cusack, S., Tidor, B. & Karplus, M. (1990). *J. Chem. Phys.* **93**, 2974–2991.
Sun, Y., Zhu, Z., Chen, S., Balakrishnan, J., Abbott, D., Ahuja, A. T. & Pickwell MacPherson, E. (2012). *Plos One*, **7**, e50306.
Tarek, M. & Tobias, D. J. (2002). *Phys. Rev. Lett.* **88**, 138101.
Tsai, A. M., Neumann, D. A. & Bell, L. N. (2000). *Biophys. J.* **79**, 2728–2732.
Tych, K. M., Burnett, A. D., Wood, C. D., Cunningham, J. E., Pearson, A. R., Davies, A. G. & Linfield, E. H. (2011). *J. Appl. Cryst.* **44**, 129–133.
Uhd Jepsen, P. & Fischer, B. M. (2005). *Opt. Lett.* **30**, 29–31.
Vinh, N. Q., Allen, S. J. & Plaxco, K. W. (2011). *J. Am. Chem. Soc.* **133**, 8942–8947.
Weik, M. (2003). *Eur. Phys. J. E*, **12**, 153–158.
Weik, M. & Colletier, J.-P. (2010). *Acta Cryst.* D**66**, 437–446.
Weik, M., Schreurs, A. M. M., Leiros, H.-K. S., Zaccai, G., Ravelli, R. B. G. & Gros, P. (2005). *J. Synchrotron Rad.* **12**, 310–317.
Weik, M., Vernede, X., Royant, A. & Bourgeois, D. (2004). *Biophys. J.* **86**, 3176–3185.
Whitmire, S. E., Wolpert, D., Markelz, A. G., Hillebrecht, J. R., Galan, J. & Birge, R. R. (2003). *Biophys. J.* **85**, 1269–1277.
Wood, K., Frölich, A., Paciaroni, A., Moulin, M., Härtlein, M., Zaccai, G., Tobias, D. J. & Weik, M. (2008). *J. Am. Chem. Soc.* **130**, 4586–4587.
Wood, K., Tobias, D. J., Kessler, B., Gabel, F., Oesterhelt, D., Mulder, F. A. A., Zaccai, G. & Weik, M. (2010). *J. Am. Chem. Soc.* **132**, 4990–4991.
Young, A. C. M., Tilton, R. F. & Dewan, J. C. (1994). *J. Mol. Biol.* **235**, 302–317.
Zhang, C., Tarhan, E., Ramdas, A. K., Weiner, A. M. & Durbin, S. M. (2004). *J. Phys. Chem. B*, **108**, 10077–10082.
Zhong, H., Redo-Sanchez, A. & Zhang, X. C. (2006). *Opt. Express*, **14**, 9130–9141.